International Journal of Engineering and Management Research e-ISSN: 2250-0758 | p-ISSN: 2394-6962
Volume-11, Issue-3 (June 2021)
www.ijemr.net https://doi.org/10.31033/ijemr.11.3.7

Design and CFD Simulation of Tesla Pump

SMG Akele[1], M. O. Ahmed[2], S. J. Wodah[3], J. Agbajor[4], K. O. Ihwurighwre[5] and O. Uwumagbuhun[6]
[1]Lecturer, Mechanical Engineering Department, Auchi Polytechnic, Auchi, NIGERIA
[2]Graduate Student, Mechanical Engineering Department, Auchi Polytechnic, Auchi, NIGERIA
[3]Student, Mechanical Engineering Department, Auchi Polytechnic, Auchi, NIGERIA
[4]Student, Mechanical Engineering Department, Auchi Polytechnic, Auchi, NIGERIA
[5]Student, Mechanical Engineering Department, Auchi Polytechnic, Auchi, NIGERIA
[6]Student, Mechanical Engineering Department, Auchi Polytechnic, Auchi, NIGERIA

[1]Corresponding Author: smg_sam2009@yahoo.com

ABSTRACT

The need for high pump performance and efficiency continue to encourage the study of flow between two parallel co-rotating discs in multiple discs pump or turbine. Therefore, this study entails the design, construction and CFD simulation of a 3D Tesla pump model axisymmetric swirling flow in order to enhance the understanding of Tesla pump for future development.

Method of solution entails designing and construction of a small prototype tesla pump and then using the design geometry and parameters to design and perform numerical simulation. The results of the numerical simulation were then analyzed.

The result obtained indicates static pressure to have minimum value of -4.7791Pa at the outlet and 13.777Pa at the pump inlet and with velocity magnitude having minimum velocity of 0.00m/s and maximum velocity of 4.12m/s. The strength of the velocity was seen to be very high at the pump outlet. The analysis radial velocity showed minimum value of -0.508m/s and maximum value of 3.981m/s with the radial velocity vector being concentrated at the discs periphery and outlet.

Model simulation results exhibited smooth pressure and velocity profiles. With the 3D simulation all flow variables are able to be predicted.

***Keywords*--** Numerical Simulation, Radial Velocity, Static Pressure, Design Models, Swirling Flow

I. INTRODUCTION

Tesla pump consists of smooth closely-spaced discs that are arranged parallel to each other along a shaft. Tesla pump operates with working medium (fluid) entering the holes around the shaft into the space between any two disc, from where it swirling radially towards discs periphery.(Akele and Akpobi, 2019).Research interest has led to categorizing the study of flow of fluid in Tesla turbo-machines into two main configurations: turbine and pump configurations. These are further categorized into radial inflow or outflow, with or without swirling, between two closely spaced parallel discs. (Eshita, 2014).The Tesla pump configuration, also referred to as a swirling outflow system, is found in applications such centrifugal compressor and gas turbine combustor.

The low efficiency challenge of Tesla pump has led to the continued research studies and experimental investigations of flow within two parallel discs gap with the intention of understanding all the inherent characteristics and phenomena surrounding flows in the gap between discs in a Tesla pump or turbine, especially for the purpose of design. Understanding of flow characteristics between parallel discs will enhance Tesla turbo-machine design for high efficiency.

Eshita (2014) used ANSYS Fluent 12.1 to numerically investigate sink and source flow between the gaps of two discs. Comparison of experimental result and numerical results obtained were observed to agree. Pandey et al. (2014) designed and simulated 1 kW Tesla turbine. In the study, high efficiencies were obtained at very low flow rates and the efficiencies are expected to be below 40%. Lampart and Jedrzejewski (2011) designed and performed analysis on a 20kW Tesla bladeless turbine for micro-power plant. The calculation domains for the investigated models of Tesla micro-turbines were done using the software Gambit. Optimal results were obtained for a model with two nozzles, 100 inlet angle and 9000 rpm and obtained efficiency was above 50% at the nominal load for mass flow rate of 100mm.Taamneh (2010) used FLUENT 6.2 a CFD software that uses FVM to solve governing equations. It was observed that high angular velocity of filter was likely to generate back pressure. The results obtained indicated that simulation results and the experimental results closely agree, which validated the software FLUENT. Tao (2014) used direct numerical simulations to investigate open Von Karman swirling flow. It was observed that the highest pressure was located near the chamber wall while the lowest pressure was located near the axial suction. And the range of pressure values were observed to increase with increase in inlet flow rate. Habhab et al. (2016) investigated micro-fluidic Tesla pump. The result of the investigation showed pressure of

This Work is under Creative Commons Attribution-NonCommercial-NoDerivatives 4.0 International License.

e-ISSN: 2250-0758 | p-ISSN: 2394-6962
Volume-11, Issue-3 (June 2021)
https://doi.org/10.31033/ijemr.11.3.7

253Pa to be generated at rotational speed of 1200rpm compared to 200Pa generated by equivalent micro-fluidic bladed turbine at 4000rpm. Power output of 53μW at 15cm resistance was generated.

II. NUMERICAL METHOD

The partial differential equations governing fluid flows of this study are the known non-linear continuity and Navier-Stokes equations that completely describe the flow of Newtonian fluids. Finite element method (FEM), finite volume method (FVM) and finite difference method (FDM) are few of the numerical technique for solving partial differential equations (PDEs) with the ability to discretized and approximate the governing equations and physical geometry model of a physical phenomenon. These coupled and nonlinear continuity and Navier-Stokes equations are solved using CFD software by applying relevant assumptions and appropriate boundary conditions. (Akpobi and Akele, 2016).

III. METHODOLOGY

Pump configuration is basically a swirling inflow configuration with the fluid entering at the disc periphery, and swirling inwards towards the discs centerline (outlet). The fluid flow domain geometry is modeled in 3D Cartesian coordinates with origin at O, Fig. 1.

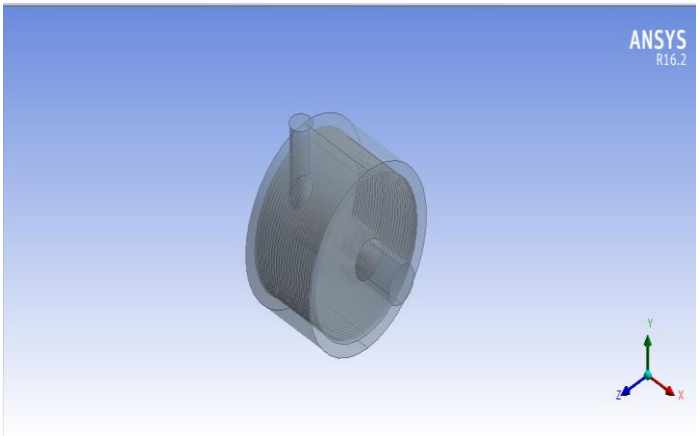

Figure 1: 3D model geometry

IV. DOMAIN DISCRETIZATION

The fluid flow domain was discretized using quadrilateral elements. The domain is subdivided into quadrilateral elements mesh along the x- and y-axes respectively, Fig. 2.

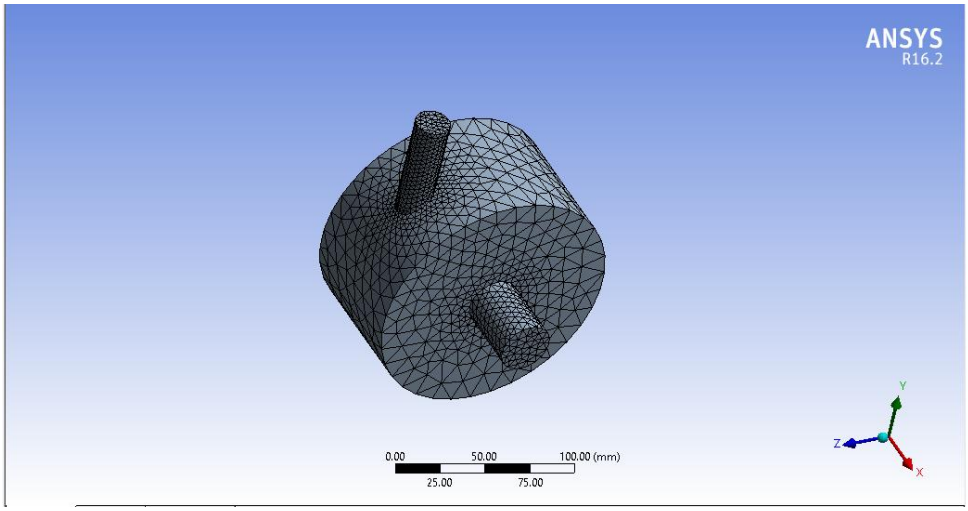

Figure 2: 3D model discretization

This Work is under Creative Commons Attribution-NonCommercial-NoDerivatives 4.0 International License.

e-ISSN: 2250-0758 | p-ISSN: 2394-6962
Volume-11, Issue-3 (June 2021)
https://doi.org/10.31033/ijemr.11.3.7

V. GOVERNING EQUATIONS

For this study, flow of fluid between the two discs is governed by the following C-NS equations (1), (2), (3) and (4) in Cartesian coordinates (Akele and Akpobi, 2019):

Continuity and Navier-Stokes equations

$$\frac{\partial u}{\partial x}+\frac{\partial u}{\partial y}+\frac{\partial u}{\partial z}=0 \quad \text{.....(1)}$$

$$\text{x: } \rho\left(\frac{\partial u}{\partial t}+u\frac{\partial u}{\partial x}+v\frac{\partial u}{\partial y}+w\frac{\partial u}{\partial z}\right)=-\frac{\partial p}{\partial x}+\mu\left(\frac{\partial^2 u}{\partial x^2}+\frac{\partial^2 u}{\partial y^2}+\frac{\partial^2 u}{\partial z^2}\right)+\rho g_x \quad \text{.....(2)}$$

$$\text{y: } \rho\left(\frac{\partial v}{\partial t}+u\frac{\partial v}{\partial x}+v\frac{\partial v}{\partial y}+w\frac{\partial v}{\partial z}\right)=-\frac{\partial p}{\partial y}+\mu\left(\frac{\partial^2 v}{\partial x^2}+\frac{\partial^2 v}{\partial y^2}+\frac{\partial^2 v}{\partial z^2}\right)+\rho g_y \quad \text{.....(3)}$$

$$\text{z: } \rho\left(\frac{\partial w}{\partial t}+u\frac{\partial w}{\partial x}+v\frac{\partial w}{\partial y}+w\frac{\partial w}{\partial z}\right)=-\frac{\partial p}{\partial z}+\mu\left(\frac{\partial^2 w}{\partial x^2}+\frac{\partial^2 w}{\partial y^2}+\frac{\partial^2 w}{\partial z^2}\right)+\rho g_z \quad \text{.....(4)}$$

VI. RELEVANT ASSUMPTIONS

Continuity and Navier-Stokes equations (1) through (4) are simplified to close-formed equations (5) through (8) respectively by applying the following assumptions. (Akele and Akpobi, 2019):

(i) Flow is incompressible, steady, and viscous flow.
(ii) Flow is analyzed in 3D.
(iii) Flow is radially inwards and symmetrical over z-coordinate.
(iv) Very large discs radius is used compared to small gap.
(v) Body forces (gravitational and inertia) are negligible,
(vi) No-slipboundary condition at discs-fluid interfaces.

VII. BOUNDARIES GEOMETRY AND BOUNDARY CONDITIONS

Considering the geometry of Fig. 3, the fluid entering at the inlet, comes in contact with both discs surface. Thus, velocity gradient is set up in the boundary layer with no-slip boundary condition between disc and fluid interface with the viscous drag in the flow domain also setting up a swirling radial inward flow in the fluid.

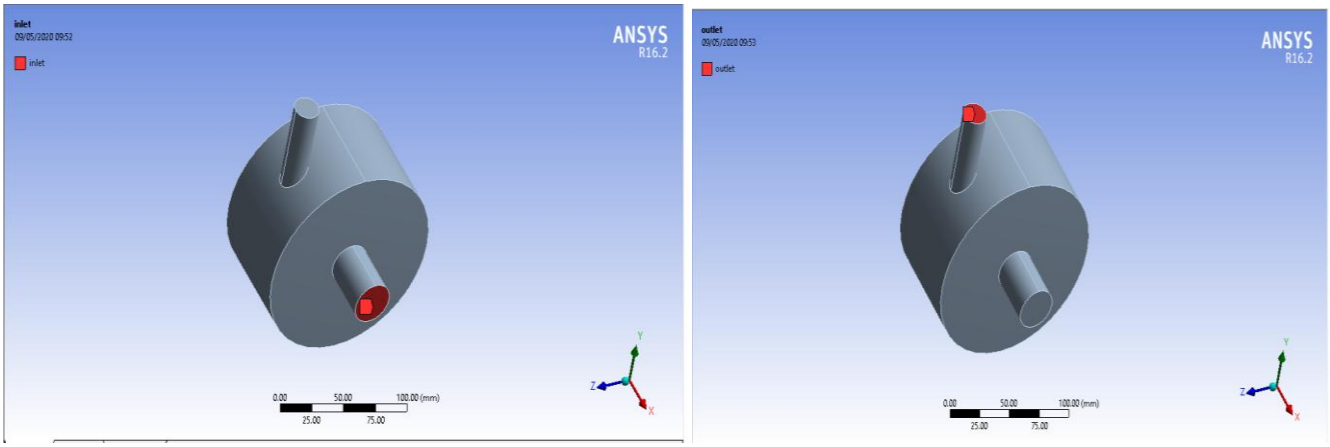

Figure 3: Boundary conditions

VIII. METHODOLOGY

The pump configuration is basically a swirling outflow configuration with the fluid entering at the disc center, swirling outwards towards the discs periphery.

8.1 Physical Model Design

The physical design involved the purchase of cylindrical plastic for housing, plexiglass for body panels, 12mm by 80mm aluminum rod for shaft, 25 plastic discs,

This Work is under Creative Commons Attribution-NonCommercial-NoDerivatives 4.0 International License.

e-ISSN: 2250-0758 | p-ISSN: 2394-6962
Volume-11, Issue-3 (June 2021)
https://doi.org/10.31033/ijemr.11.3.7

two bearings, water hoses, electric motor, 11 bolts and nuts, washers, pvc pipe, and super glue shown in Fig. 4.

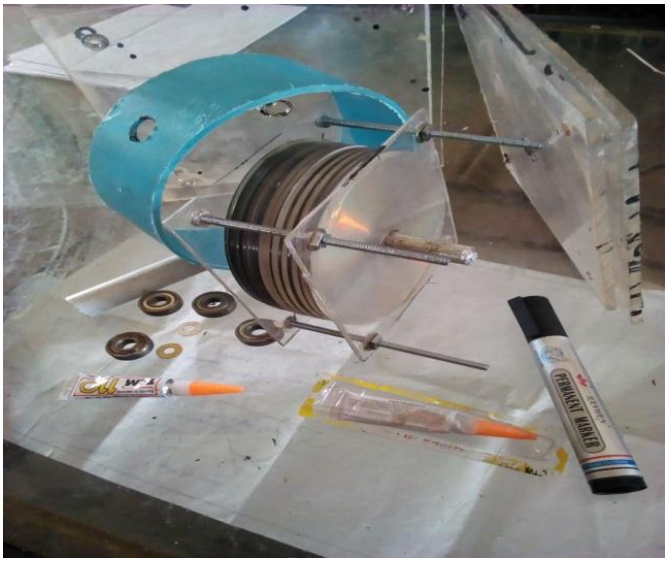

Figure 4: Physical model parts

The plastic and plexiglass were cut to design sizes; the aluminum rod was machined according to design requirement to carry the discs and the bearings at both ends; holes were drilled around the discs, with the disc center hole as fluid outlet.

Table 1: Physical model parameters

Parameters	Symbols	model value
Outer radius	r_o	120mm
Inner radius	r_i	30mm
Disc gap	B	1mm
Disc thickness	T	2mm
Casing (stator)inner diameter	D_i	140mm
No of spacers	S	32units
No of disc	C	31units
Angular velocity	ω (average)	1800rpm
Height	h	500mm
Width	w	500mm
Length	L	500mm
Mass	M	12kg

8.2 Model Simulation

The design model was simulated by using Fluent Fluid Flow Design Modeler bench to generate the model mesh while the Fluent Solver was used to analyze. The 3D analysis was set up on 3D space, pressure-based, viscous, steady and axisymmetric swirling flow with air as the working medium, pressure 0 pascal; moving wall, no-slip; rotational velocity – 1800 rpm.

In this study, Akele et al. (2021) turbine design static pressure, velocity magnitude and radial velocity results are compared analytically since the same design parameters were used for both models. The obtained values are shown in Table 3.

This Work is under Creative Commons Attribution-NonCommercial-NoDerivatives 4.0 International License.

e-ISSN: 2250-0758 | p-ISSN: 2394-6962
Volume-11, Issue-3 (June 2021)
https://doi.org/10.31033/ijemr.11.3.7

Table 2: Simulation model parameters

Parameters		Symbols	Simulation value
Outer radius		r_o	120mm
Inner radius		r_i	30mm
Disc gap		B	1mm
Disc thickness		T	2mm
Casing inner diameter		D_i	140mm
Boundary conditions:	inlet	m_i	0.001kg/s
	outlet	p_g	0pascal
Turbulence model		-	K-epsilon
Mass flow rate		m_o	7.2kg/s
No of spacers		S	32units
No of disc		C	31units
Angular velocity		Ω	1800rpm
Height		H	140mm
Width		W	140mm
Length		L	140mm

Tables 3: Tables show values of pump design and turbine design (Akele et al., 2021)

Distance (mm)	Pump static pressure (pa)	Turbine static pressure (pa)
0	13.8	94.6
0.1	12.8	89.5
0.2	11.9	84.4
0.3	11	79.3
0.4	10.1	74.2
0.5	9.13	69.1
0.6	8.22	64
0.7	7.28	58.9
0.8	6.5	53.8
0.9	5.42	48.8
1	4.49	43.7
1.1	3.56	38.6
1.2	2.54	33.5
1.3	1.71	28.4
1.4	0.78	23.3
1.5	-0.15	18.2
1.6	-1.08	13.1
1.7	-2.01	8.01
1.8	-2.93	2.91
1.9	-3.86	-2.18
2	-4.79	-7.28

Distance (mm)	Pump velocity magnitude (m/s)	Turbine velocity magnitude (m/s)
0	0	0
0.1	0.21	0.96
0.2	0.41	1.92
0.3	0.62	2.88
0.4	0.82	3.85
0.5	1.03	4.81
0.6	1.23	5.77
0.7	1.44	6.73
0.8	1.65	7.69
0.9	1.85	8.65
1	2.06	9.62
1.1	2.26	10.6
1.2	2.47	11.5
1.3	2.68	12.5
1.4	2.88	13.5
1.5	3.09	14.4
1.6	3.29	15.4
1.7	3.5	16.3
1.8	3.7	17.3
1.9	3.91	18.3
2	4.12	19.2

Distance (mm)	Pump radial velocity m/s)	Turbine Radial velocity (m/s)
0	-0.51	-7.3
0.1	-0.29	-6.55
0.2	-0.07	-5.81
0.3	0.15	-5.06
0.4	0.37	-4.31
0.5	0.6	-3.56
0.6	0.81	-2.81
0.7	1.03	-2.06
0.8	1.25	-1.32
0.9	1.47	-0.57
1	1.69	0.18
1.1	1.91	0.93
1.2	2.13	1.68
1.3	2.35	2.43
1.4	2.57	3.17
1.5	2.79	3.92
1.6	3.01	4.67
1.7	3.23	5.42
1.8	3.45	6.17
1.9	3.67	6.92
2	3.89	7.66

This Work is under Creative Commons Attribution-NonCommercial-NoDerivatives 4.0 International License.

e-ISSN: 2250-0758 | p-ISSN: 2394-6962
Volume-11, Issue-3 (June 2021)
https://doi.org/10.31033/ijemr.11.3.7

IX. RESULTS AND DISCUSSION

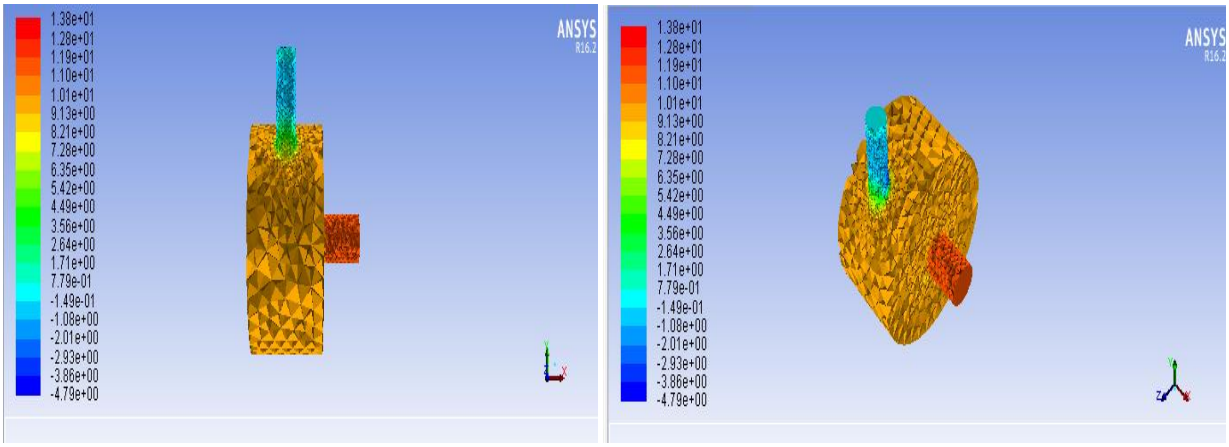

Figure 5: 3D view for static pressure contour

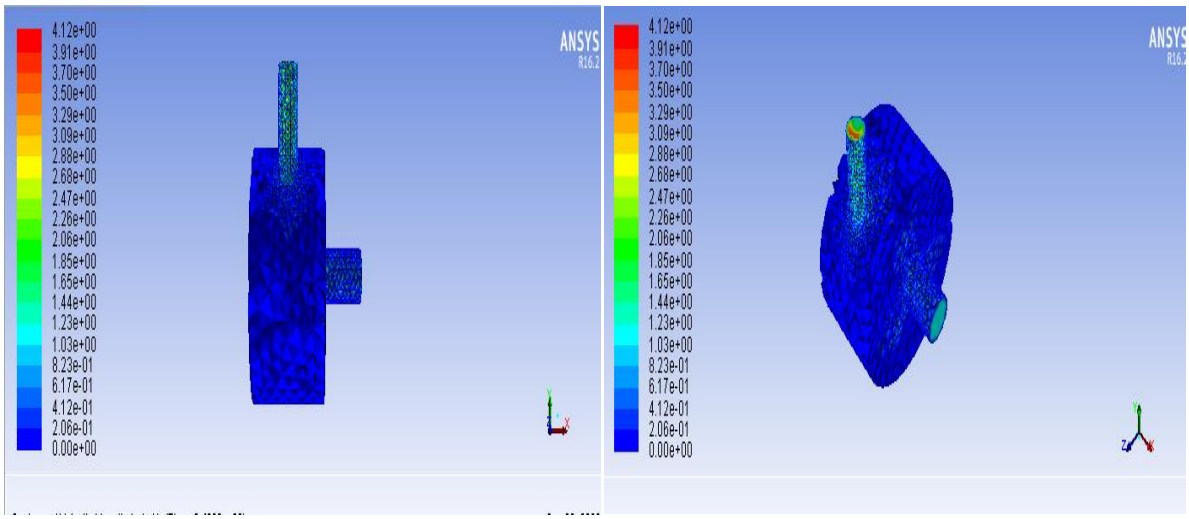

Figure 6: Contour of velocity magnitude

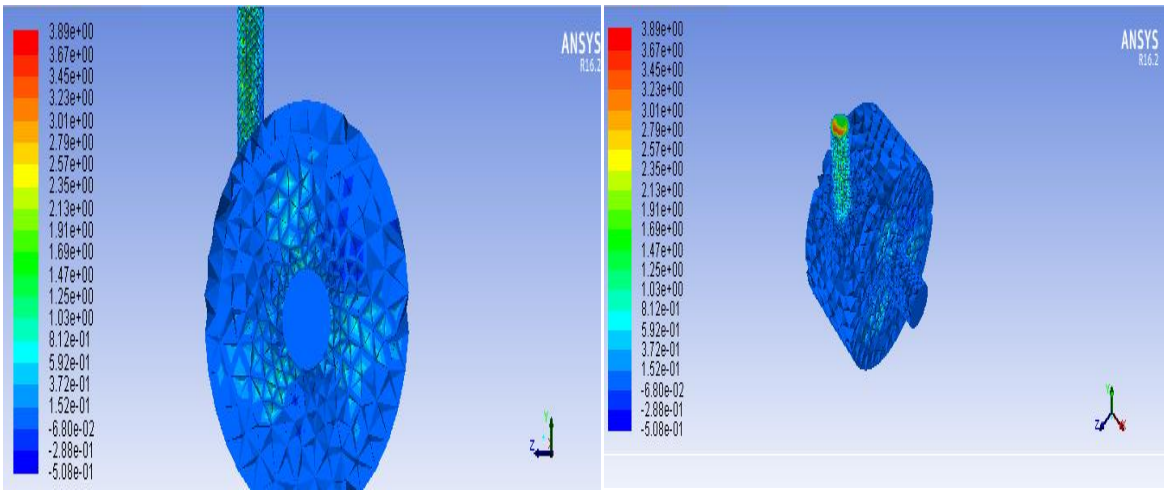

Figure 7: Radial velocity vector

This Work is under Creative Commons Attribution-NonCommercial-NoDerivatives 4.0 International License.

e-ISSN: 2250-0758 | p-ISSN: 2394-6962
Volume-11, Issue-3 (June 2021)
https://doi.org/10.31033/ijemr.11.3.7

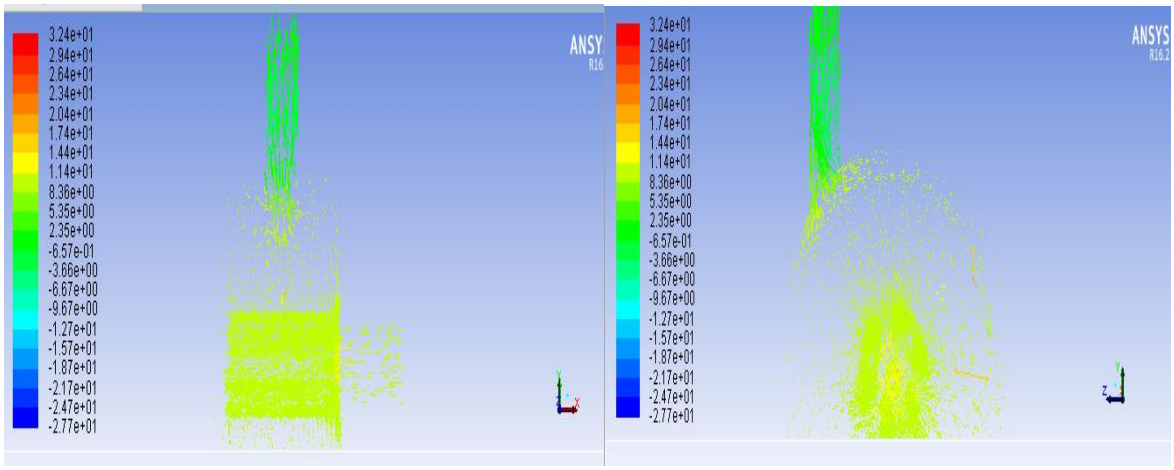

Figure 8: Pressure velocity vector

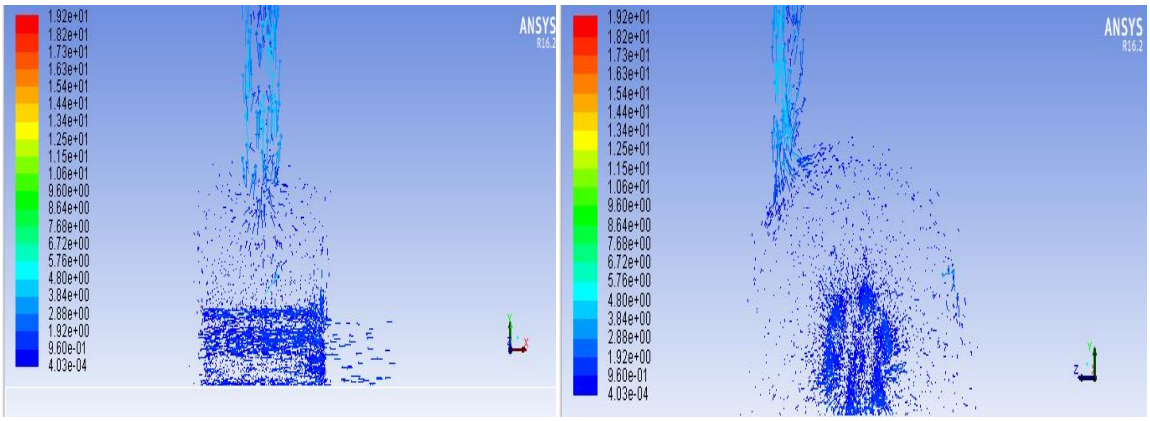

Figure 9: Velocity magnitude vector

Post- Processing Results

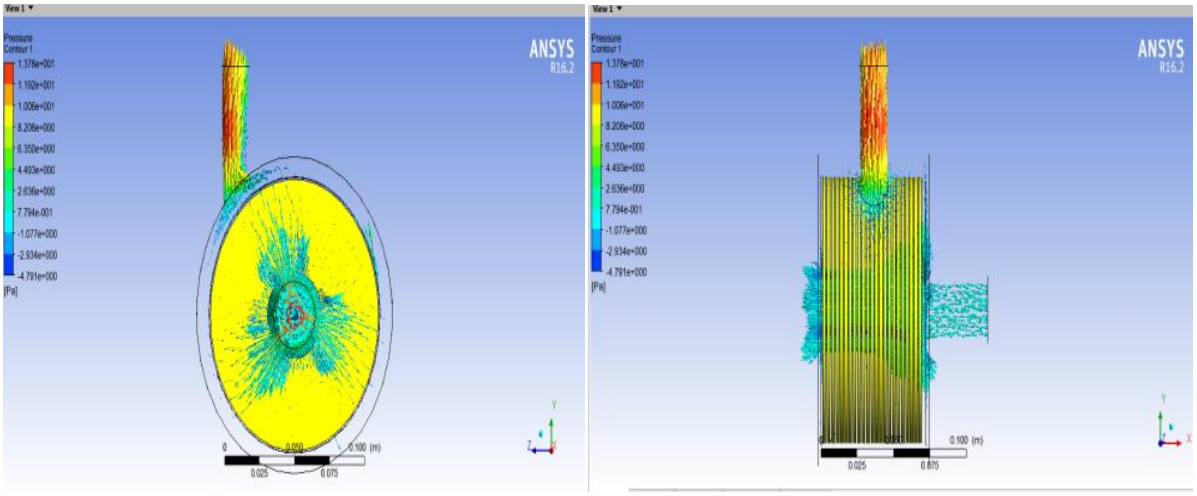

Figure 10: Static pressure

This Work is under Creative Commons Attribution-NonCommercial-NoDerivatives 4.0 International License.

e-ISSN: 2250-0758 | p-ISSN: 2394-6962
Volume-11, Issue-3 (June 2021)
https://doi.org/10.31033/ijemr.11.3.7

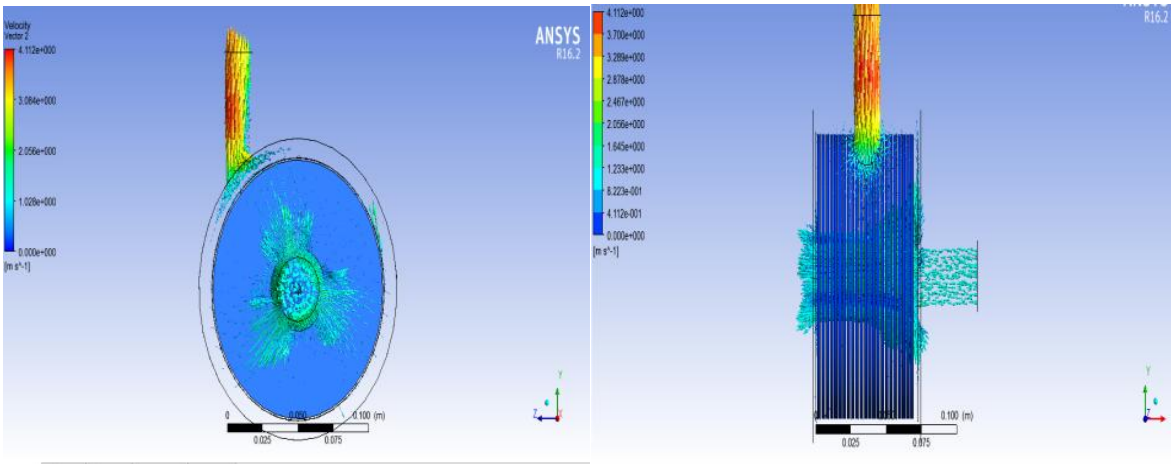

Figure 11: Velocity vector

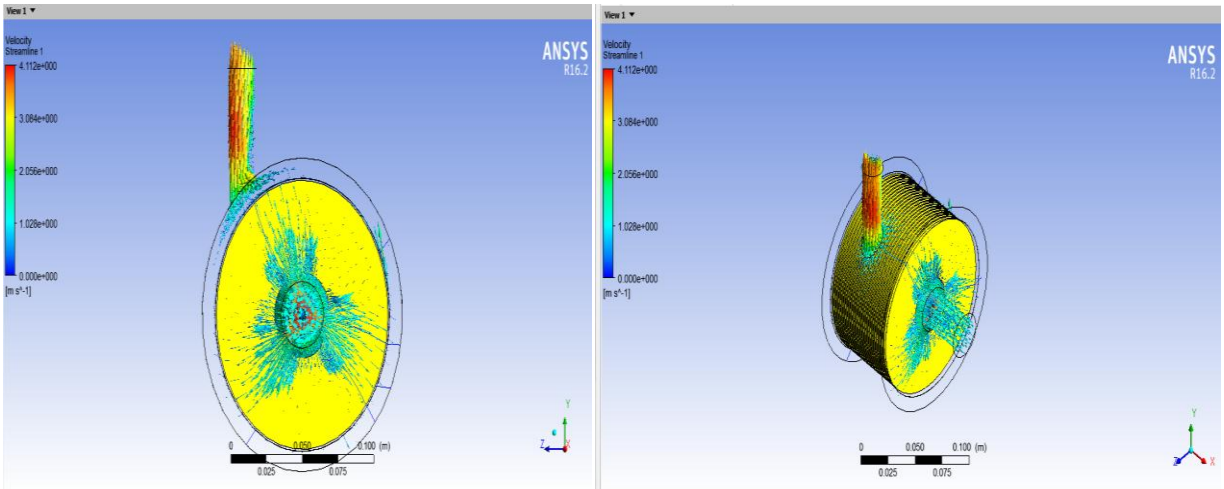

Figure 12: Velocity streamline

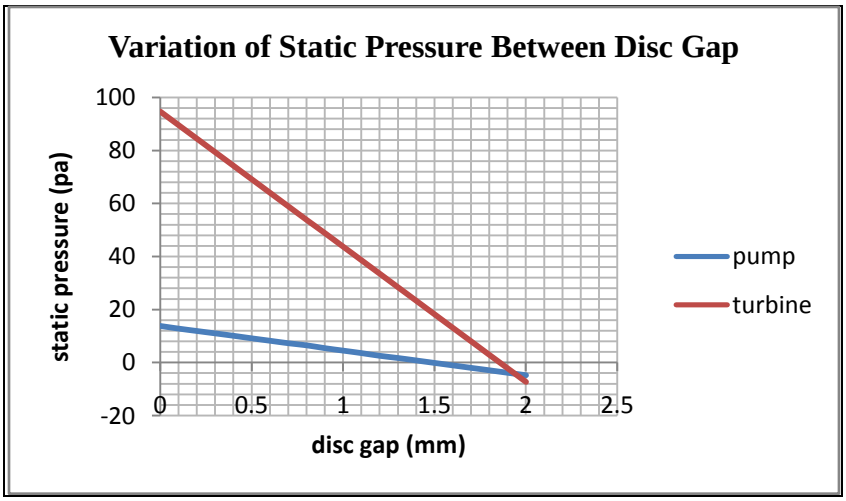

Figure 13: Pump and turbine static pressures

This Work is under Creative Commons Attribution-NonCommercial-NoDerivatives 4.0 International License.

e-ISSN: 2250-0758 | p-ISSN: 2394-6962
Volume-11, Issue-3 (June 2021)
https://doi.org/10.31033/ijemr.11.3.7

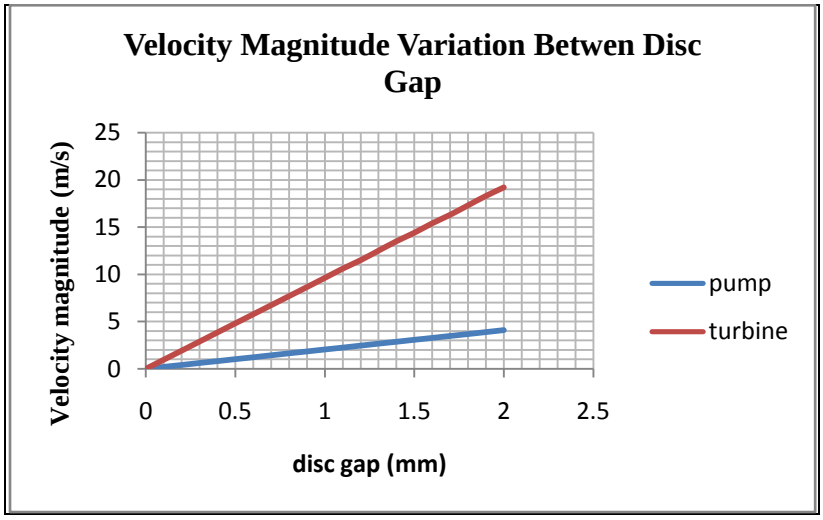

Figure 14: Pump and turbine velocity magnitudes

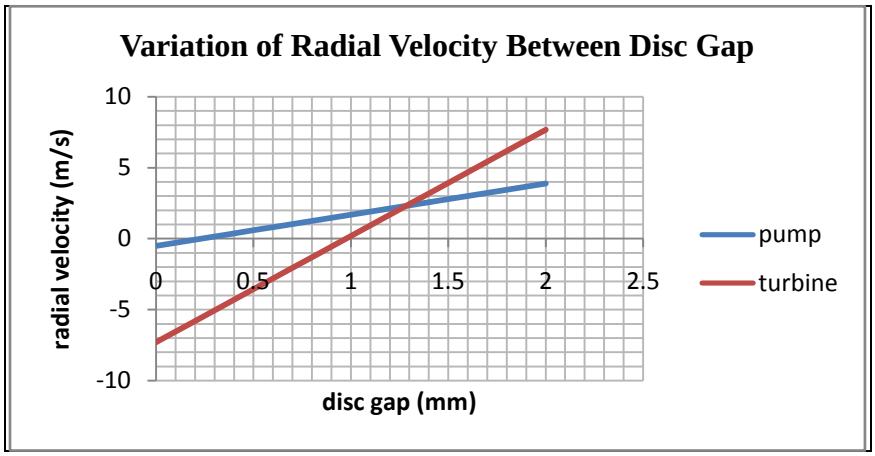

Figure 15: Pump and turbine radial velocities

Fig. 5 shows 3D view for static pressure contour, which is seen to have minimum value of -4.7791Pa at the outlet and 13.777Pa at the pump inlet. Fig. 6 shows contour of velocity magnitude with minimum velocity of 0.00m/s and maximum velocity of 4.12m/s. The strength of the contour is seen to be very high at the pump outlet. Fig. 7 shows pump radial velocity vector with minimum value of -0.508m/s and maximum value of 3.981m/s; the radial velocity vector is seen to be concentrated at the discs periphery and outlet. Fig. 8 depicts pump pressure velocity vector with minimum velocity of -27.709m/s and maximum velocity of 32.407m/s; the velocity vector is seen to be concentrated at the in the discs gap and near the centre. Fig. 9 depicts pump velocity magnitude vector with minimum velocity of 0.0004m/s and maximum velocity of 19.189m/s; the velocity vector is seen to be concentrated at the discs periphery and outlet.

Fig. 10 through Fig. 12 show post-processing results of the simulation. Fig. 10 shows pump static pressure with minimum velocity of -4.791Pa and maximum velocity of 10.378Pa. Fig. 11 depicts pump velocity vector with minimum velocity of .00m/s and maximum velocity of 4.11m/s; the velocity vector is seen to be high near the outlet. Fig.12 shows the result of the velocity streamline.

Fig. 13 shows the present study pump design and turbine design Akele et al. (2021) plot of static pressure. Though both decrease linearly from 94.6pa and 13.8pa to -7.28pa and -4.79pa respectively, it is revealed that pressure is very low at pump design inlet while high at turbine design inlet (this validated pump and turbine design output). Fig. 14 is present study and Akele et al. (2021) plots of velocity magnitude against disc gap. The velocities are seen to increase linearly and proportionately from 0.0 m/s and 0.0 m/s to 4.12 m/s and 19.2 m/s respectively. Fig.

This Work is under Creative Commons Attribution-NonCommercial-NoDerivatives 4.0 International License.

15 is present study and Akele et al. (2021) plot of radial velocity between any two discs surfaces with minimum and maximum velocities of -0.51m/s and -7.30m/s to 3.89 and 7.66m/s respectively. All the curves in Fig. 13, Fig 14 and Fig. 15 satisfy initial inlet and boundary conditions of the design models.

X. CONCLUSION

A prototype Tesla pump was designed and CFD simulation performed based on the parameters. Model simulation results exhibited smooth pressure and velocity profiles and satisfied initial and boundary conditions. With the 3D simulation all flow variables can be predicted.

REFERENCES

[1] Akele, S.M.G. & Akpobi, J. A. (2019). Numerical simulation of flow between two parallel co-rotating discs. *International Journal of Engineering and Management Research, 9*(6), 13–22.

[2] Akele1 et al. (2021). Design, construction and simulation of tesla turbine. *International Journal of Engineering and Management Research, 11*(1), 84–92.

[3] Eshita, I. J. (2014). Turbulence modeling of source and sink flows. *International Journal of Mechanical, Aerospace, Industrial, Mechatronic and Manufacturing Engineering, 8*(5), 821-826.

[4] Habhab, M., Ismail, T., & Lo, J. F. (2016). A laminar flow-based micro-fluidic tesla pump via lithography enabled 3D printing. *Sensors, 16*, 1-10.

[5] Lampart, P. & Jędrzejewski, L. (2011). Investigations of aerodynamics of tesla bladeless micro-turbines. *Journal of Theoretical and Applied Mechanics, 49*(2), 477-499.

[6] Pandey, R., Pudasaini, S., Saurav, D., Uprety, R. B., & Dr. Neopane, H. P. (2014). Design and computational analysis of 1kw tesla turbine. *International Journal of Scientific and Research Publications, 4*(11), 1-5.

[7] Taamneh, Y. (2010). Numerical simulation of fluid flow in enclosed rotating filter and disk. *ARPN Journal of Engineering and Applied Sciences, 5*(9), 48-53.

[8] Tao, X. (2014). Direct numerical simulation of open Von Karman swirling flow. *Journal of Hydrodynamics, 26*(2), 165-177.

This Work is under Creative Commons Attribution-NonCommercial-NoDerivatives 4.0 International License.